# Dominant role by vertical wind shear in regulating aerosol effects on deep convective clouds

Jiwen Fan,[1] Tianle Yuan,[2,3] Jennifer M. Comstock,[1] Steven Ghan,[1] Alexander Khain,[4] L. Ruby Leung,[1] Zhanqing Li,[5] Vanderlei J. Martins,[2,3] and Mikhail Ovchinnikov[1]

Received 28 April 2009; revised 25 August 2009; accepted 15 September 2009; published 24 November 2009.

[1] Aerosol-cloud interaction is recognized as one of the key factors influencing cloud properties and precipitation regimes across local, regional, and global scales and remains one of the largest uncertainties in understanding and projecting future climate changes. Deep convective clouds (DCCs) play a crucial role in the general circulation, energy balance, and hydrological cycle of our climate system. The complex aerosol-DCC interactions continue to be puzzling as more "aerosol effects" unfold, and systematic assessment of such effects is lacking. Here we systematically assess the aerosol effects on isolated DCCs based on cloud-resolving model simulations with spectral bin cloud microphysics. We find a dominant role of vertical wind shear in regulating aerosol effects on isolated DCCs, i.e., vertical wind shear qualitatively determines whether aerosols suppress or enhance convective strength. Increasing aerosols always suppresses convection under strong wind shear and invigorates convection under weak wind shear until this effect saturates at an optimal aerosol loading. We also found that the decreasing rate of convective strength is greater in the humid air than that in the dry air when wind shear is strong. Our findings may resolve some of the seemingly contradictory results among past studies by considering the dominant effect of wind shear. Our results can provide the insights to better parameterize aerosol effects on convection by adding the factor of wind shear to the entrainment term, which could reduce uncertainties associated with aerosol effects on climate forcing.

**Citation:** Fan, J., T. Yuan, J. M. Comstock, S. Ghan, A. Khain, L. R. Leung, Z. Li, V. J. Martins, and M. Ovchinnikov (2009), Dominant role by vertical wind shear in regulating aerosol effects on deep convective clouds, *J. Geophys. Res.*, *114*, D22206, doi:10.1029/2009JD012352.

## 1. Introduction

[2] Aerosol effects on clouds have great potential to affect the radiative balance of our atmosphere and the hydrological cycle, yet they remain one of the least understood aspects of climate science [*National Research Council*, 2005]. Although relatively consistent results have been reached for aerosol effects on droplet number concentration and cloud albedo for warm clouds and stratocumulus [e.g., *Albrecht*, 1989; *Kaufman et al.*, 2005], there are still large disagreements on the influence of aerosols on liquid water path [e.g., *Ackerman et al.*, 2004; *Guo et al.*, 2008]. The effect of relative dispersion and its representation is even more inconsistent and underexplored [*Liu and Daum*, 2002; *Liu et al.*, 2006; *Lu et al.*, 2007; *Liu et al.*, 2008]. Our understanding of aerosol–deep convective clouds is even poorer. Aerosol effects on deep convective clouds (DCCs) as from both observational and model studies have indicated that aerosol may either suppress convection and precipitation [*Rosenfeld*, 1999, 2000; *Khain et al.*, 2004; *Khain and Pokrovsky*, 2004] or enhance convection and precipitation [*Khain et al.*, 2005, 2008; *Fan et al.*, 2007b; *Lin et al.*, 2006; *van den Heever et al.*, 2006; *Zhang et al.*, 2007]. *Lin et al.* [2006] found that statistically aerosols seem to increase precipitation over the Amazon region based on multisatellite data sets while case studies by *Rosenfeld* [1999, 2000] clearly show suppressing effects. *Koren et al.* [2008] found an optimum cloud condensation nucleus concentration (CCNC) as approximated by aerosol optical depth through analysis of observational data. *Rosenfeld et al.* [2008] arrived at a similar conclusion that aerosols can first enhance convective strength, then reach an optimum concentration and suppress convective strength based on a simple parcel model calculation as aerosol increases. They also concluded that aerosols could increase or suppress

[1]Climate Physics Group, Pacific Northwest National Laboratory, Richland, Washington, USA.
[2]Climate Branch, NASA Goddard Space Flight Center, Greenbelt, Maryland, USA.
[3]Joint Center for Earth Systems Technology, University of Maryland Baltimore County, Baltimore, Maryland, USA.
[4]Institute of Earth Science, Hebrew University of Jerusalem, Jerusalem, Israel.
[5]Department of Atmospheric and Oceanic Sciences and Earth System Science Interdisciplinary Center, University of Maryland at College Park, College Park, Maryland, USA.

Copyright 2009 by the American Geophysical Union.
0148-0227/09/2009JD012352

precipitation depending on specific conditions. Model simulations also produce seemingly opposite effects of aerosols on convection and precipitation [*Khain and Pokrovsky*, 2004; *Teller and Levin*, 2006; *Wang*, 2005; *Fan et al.*, 2007b; *van den Heever et al.*, 2006]. An optimum cloud condensation nuclei (CCN) concentration was also found in some cloud-resolving model (CRM) studies in terms of enhancement of convection and precipitation by aerosols [*Wang*, 2005; *Fan et al.*, 2007b].

[3] Many factors were proposed to affect how aerosols interact with convection and precipitation. Aerosol characteristics such as aerosol composition, size distribution, especially the availability of giant CCN, could significantly affect cloud nucleating properties and then convective strength [*Rudich et al.*, 2002; *Levin and Cotton*, 2008; *Fan et al.*, 2007a; *Yuan et al.*, 2008]. Relative humidity (RH) has been identified as one of the important thermodynamic factors to affect the relationship between aerosols and convection [*Fan et al.*, 2007b; *Khain et al.*, 2004, 2005, 2008; *Yuan et al.*, 2008; *Khain*, 2009]. *Khain et al.* [2008] and *Khain* [2009] attempted to classify different studies and highlighted a few factors that determine the impact of aerosols on clouds. It was found that generally aerosols suppress convection for isolated clouds formed in a relatively dry condition; aerosols invigorate convection for convective systems inside a moist environment. Wind shear was also hinted at as a potentially important factor affecting aerosol impact on precipitation. However, the effect of wind shear was largely overlooked in previous studies that investigated aerosol impact on convective clouds. It has been indicated that low-tropospheric and midtropospheric wind shear is critical in organizing mesoscale convection systems especially for squall lines [*Schoenberg Ferrier et al.*, 1996; *Takemi*, 2007]. For isolated convections, however, it can suppress cloud vertical development [*Richardson and Droegemeier*, 2007; *Byers and Battan*, 1949]. Past studies indicate the twofold role of the vertical wind shear on convection [*Khain et al.*, 2005; *Lee et al.*, 2008; *Khain*, 2009]. In case of single DCC the increase of wind shear leads to higher detrainment and evaporation of cloud hydrometeors. This effect is especially important for clouds developing in polluted air since particles are smaller and evaporate more easily in these clouds. As a result, the increase of wind shear was found to decrease precipitation in polluted clouds. At the same time, the increased wind shear leading to increased evaporation and cooling intensified downdrafts and fostered formation of secondary clouds, cloud ensembles, and squall lines [*Khain et al.*, 2005; *Tao et al.*, 2007; *Lee et al.*, 2008]. However, detailed quantitative analysis of the role of wind shear was not included in these studies.

[4] The complex aerosol-DCC interactions continue to be puzzling as more "aerosol effects" unfold, and there has been no systematic assessment of aerosol effects on deep convection under various thermodynamic and dynamical environments. This study was performed to systematically assess aerosol effects on DCCs and to find the important regulating factors determining the relationship between aerosols and convection. Note that we only explore aerosol effects on convection by serving as CCN. Aerosols may have important effects on mixed-phase or ice-phase cloud properties by serving as ice nuclei (IN) [*Sassen et al.*, 2003; *van den Heever et al.*, 2006; *Ekman et al.*, 2007], but they would not significantly modify convective strength in DCCs (J. Fan, J. M. Comstock, and M. Ovchinnikov, Dominant effects of CCN over IN on tropical anvil characteristics and water vapor of the Tropical Tropopause Layer (TTL), submitted to *Journal of Geophysical Research*, 2009). Using simulations of a CRM with a detailed bin microphysics, we report here a dominant role of wind shear in determining the response of convection to increasing CCNC. To simplify the problem, we concentrated here on isolated DCCs, which are relatively simple dynamically and mainly driven by surface moisture and heat fluxes. Isolated DCCs may have a less significant role in the global climate system than convection ensembles, but they occur much more frequently, especially during the monsoon break period. These frequently occurring isolated DCCs, often referred to as "afternoon showers," significantly affect the weather system and hydrological cycle in many regions of the world such as southeast of Texas, northeast of Australia, and Eastern China.

## 2. Methods

[5] We conducted model simulations using the two-dimensional (2-D) version of a CRM coupled with detailed spectral bin microphysics for many different isolated DCCs to find the important factors in regulating aerosol effects on isolated DCCs.

### 2.1. Model Description

[6] A cloud-resolving model, the System for Atmospheric Modeling (SAM), coupled with a spectral bin microphysical scheme (SBM) [*Fan et al.*, 2009] was employed to do the simulations. The original SBM [*Khain et al.*, 2004] is based on solving an equation system for eight number size distributions for water drops, ice crystals (columnar, plate like, and dendrites), snowflakes, graupel, hail/frozen drops, and CCN. Each size distribution is represented by 33 mass doubling bins, i.e., the mass of a particle $m_k$ in the $k$ bin is determined as $m_k = 2\ m_{k-1}$. All relevant microphysical processes and interactions including droplet nucleation, primary and secondary ice generation, condensation/evaporation of drops, deposition/sublimation of ice particles, freezing/melting, and mutual collisions between the various hydrometeors are calculated explicitly. The dependence of the collision efficiencies on height and the effects of turbulence on the rate of collisions are taken into account. An updated remapping scheme has been used that conserves three moments of the hydrometeor size distributions (concentration, mass, and radar reflectivity) to reduce spectral broadening and be more consistent with observations [*Khain et al.*, 2008]. Modifications have been made to the original SBM by *Fan et al.* [2009]. An additional size distribution has been added for IN, and a theoretical ice nucleation parameterization [*Khvorostyanov and Curry*, 2000] has been incorporated to build a link between ice nucleation and aerosol properties (size distribution, composition, etc). In addition, CCN recycling from evaporation and IN sublimation recycling from sublimation have been considered (see *Fan et al.* [2009] for details).

[7] SAM is a CRM with the dynamical framework of a large eddy simulation (LES) model and the detailed model

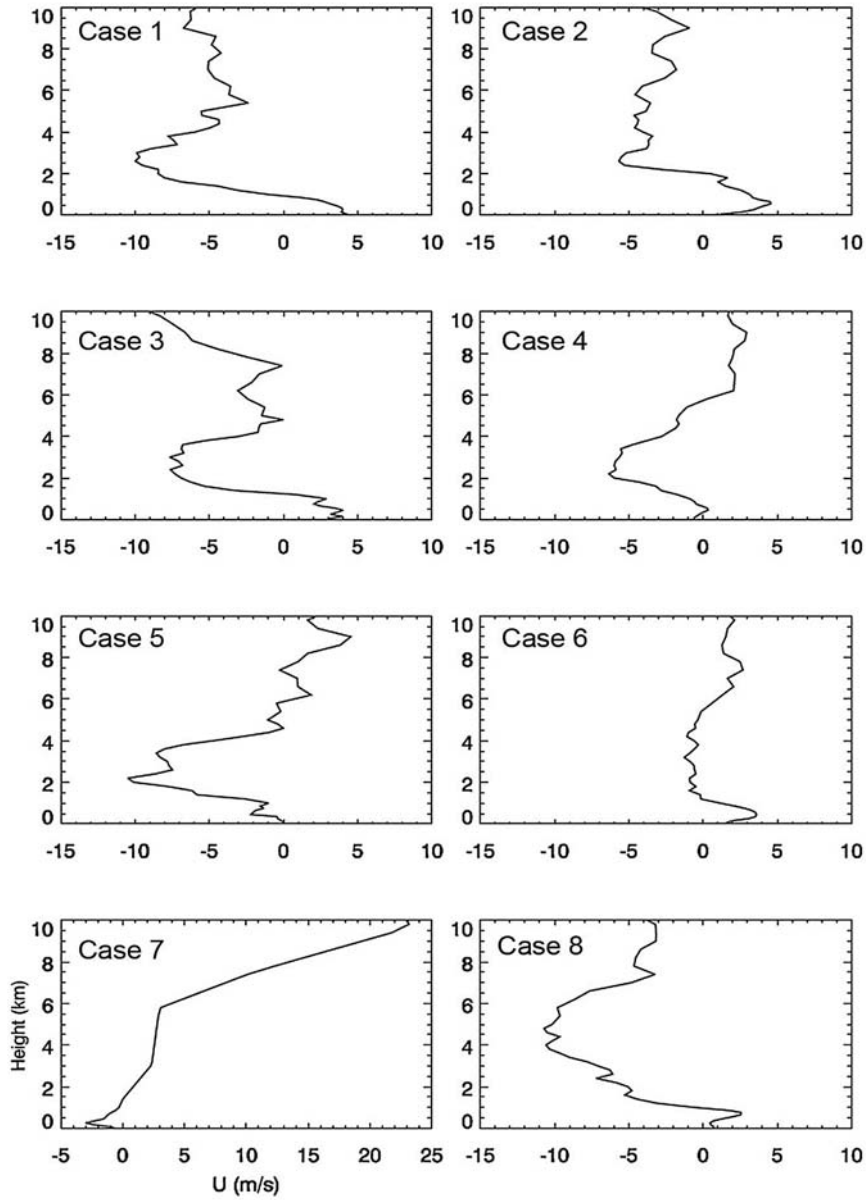


**Figure 1.** Profiles of *U* component of wind fields for eight cases shown in Table 1.

description is given by *Khairoutdinov and Randall* [2003]. Here some highlights are presented. SAM solves the equations of motion using the anelastic approximation. The finite difference representation of the model equations uses the Arakawa C staggering, with stretched vertical and uniform horizontal grids. The advection and diffusion of momentum are of second-order accuracy. Time integration of momentum equations is done using the third-order Adams-Bashforth scheme with variable time stepping to maintain linear stability. The subgrid-scale (SGS) fluxes have been parameterized with the options of a Smagorinsky-type closure and 1.5-order SGS closure based on prognostic SGS turbulent kinetic energy. Advection of all scalar prognostic variables is done using a monotonic and positive-definite advection scheme [*Smolarkiewicz and Grabowski*, 1990]. A damping layer is implemented in the upper third of the domain to reduce gravity wave reflection and buildup [*Khairoutdinov and Randall*, 2003, 2006].

### 2.2. Designs of Numerical Experiments

[8] Simulations were performed in two steps. In the first step, eight single DCCs developed in different thermodynamic, and dynamical environments were simulated. The sounding data in the eight cases shown in Table 1 were obtained from northern Australia close to Darwin during November 2005 to February 2006 and east of China near Shanghai in July 1998. For each case, simulations were performed under clean and polluted conditions with droplet concentrations of about 110–1100 $cm^{-3}$ at the cloud base, corresponding to CCNC of also about 110–1100 $cm^{-3}$, respectively, since all of CCN can be activated as cloud droplets with the specified CCN composition and size

**Table 1.** Quantities from Eight Deep Convective Cloud Cases Under the Clean and Polluted Conditions

| | Case 1 | Case 2 | Case 3 | Case 4 | Case 5 | Case 6 | Case 7 | Case 8 |
|---|---|---|---|---|---|---|---|---|
| $W$[a] (m s$^{-1}$) | | | | | | | | |
| Clean | 7.76 | 10.00 | 8.20 | 5.56 | 7.90 | 5.50 | 6.94 | 10.00 |
| Polluted | 5.95 | 8.21 | 7.50 | 5.72 | 5.47 | 6.12 | 5.76 | 6.69 |
| Liquid water[b] (g m$^{-3}$ km$^{-1}$) | | | | | | | | |
| Clean | 3.07 | 17.40 | 2.11 | 1.62 | 5.29 | 0.74 | 1.78 | 10.82 |
| Polluted | 2.26 | 12.67 | 0.71 | 1.68 | 1.85 | 0.84 | 1.13 | 2.11 |
| Ice crystal mass[b] (g m$^{-3}$ km$^{-1}$) | | | | | | | | |
| Clean | 6.94 | 31.96 | 0.97 | 2.61 | 8.23 | 1.29 | 1.38 | 6.93 |
| Polluted | 4.99 | 6.03 | 0.25 | 2.89 | 0.57 | 1.44 | 0.25 | 1.52 |
| Precipitating ice[b] (g m$^{-3}$ km$^{-1}$) | | | | | | | | |
| Clean | 8.41 | 50.21 | 1.82 | 3.68 | 10.56 | 1.47 | 2.49 | 13.58 |
| Polluted | 2.89 | 6.53 | 0.15 | 2.81 | 0.57 | 1.14 | 0.45 | 1.50 |
| Wind shear[c] (m s$^{-1}$) | 13.88 | 10.12 | 11.68 | 7.48 | 11.94 | 4.86 | 10.61 | 12.79 |
| Humidity[d] | median | humid | median | median | dry | dry | median | humid |

[a]$W$ is the averaged updraft velocity over values larger than 5 m s$^{-1}$ during the 1 h period centered at the maximum convective strength ($W_{max}$), i.e., 30 min before and after $W_{max}$.
[b]Sum over 1 h period after $W_{max}$ and divided by horizontal domain size. Precipitating ice is the sum of snow, graupel, and hail.
[c]Wind shear is calculated by max($u$) minus min($u$) within 7 km from ground. Values less than 5 m s$^{-1}$ here are thought as typical weak wind shear cases and larger than 10 m s$^{-1}$ are strong wind shear cases. Case 4 of a value 7.48 m s$^{-1}$ is a relatively weak wind shear case.
[d]Dry, median, and humid are defined with the averaged RH over 500–900 mb of <50, 50–60, and >60%, respectively.

distribution stated in the next paragraph. The profiles of wind field ($U$ component) are shown in Figure 1. It is shown that cases 4 and 6 have weak low-tropospheric or midtropospheric wind shear, but those in the other cases are strong. The surface sensible and latent heat fluxes for each case were obtained from the observations. Since we were trying to include different single DCC cases, the surface heat fluxes were expected to vary from case to case. The maximum difference in the surface latent heat fluxes among the cases is about 200 W m$^{-2}$ and the surface sensible heat fluxes vary within 10 W m$^{-2}$. From these simulations, we identify the significant factors in terms of aerosol effects in various thermodynamic and dynamic environments.

[9] In the second step, further sensitivity experiments were designed for these two cases representing the most significant increase and decrease in convective strength by aerosols to examine the relative importance of the factors identified. Four soundings were created for each of the representative cases by switching wind shear profiles and changing RH. For each sounding, four CCNC levels from 110, 220, 440, to 1100 cm$^{-3}$ were run to examine the aerosol effects. More details about the simulations conducted in this step are presented in section 3.

[10] In all simulations, the shape of aerosol size distribution was kept the same, which was taken from the aircraft measurements around Darwin, Australia [*Allen et al.*, 2008]. Aerosols over each size bin are changed by a same factor for the sensitivity tests on CCNC. An exponential decrease of aerosol concentrations with height was assumed above the boundary layer [*Khain et al.*, 2000; *Fan et al.*, 2007a, 2007b]. CCN in each bin is prognostic, and the processes considered include advection, activation, and droplet evaporation. Aerosol composition was assumed as ammonium sulfate. CCN activation was calculated using the Köhler theory which is same as *Khain et al.* [2004]. Surface sensible and latent heat fluxes were not changed in all the sensitivity tests of a specific case.

[11] Simulations described above are run on a 2-D computational domain composed of 768 horizontal grid points and 72 vertical grid points with a horizontal resolution of 300 m. Stretched vertical coordinates were used with the resolution increasing from the bottom (100 m) to top (400 m). The model top was about 24 km. Periodic lateral boundary conditions were used. The dynamic time step was 2 s. An initial heat perturbation was used to initiate convection. The intensity of the heat perturbation varied with the cases with different soundings. Simulations were run for 3 h.

## 3. Results

[12] Table 1 shows the results for the simulated eight deep convective clouds. We find that aerosol effects on DCCs respond to different cases in the following way: the averaged updraft velocity, a surrogate for convective strength, is increased by aerosols in two cases characterized by weak wind shear (cases 4 and 6) and is decreased in other cases. Liquid water mass and ice crystal mass also increase or decrease accordingly because of their strong correlation with convective strength. The most dramatic increase and decrease in updraft velocity are found for case 6 and case 8, respectively. Case 6 is characterized by weak wind shear (WWS) and a dry atmosphere, while case 8 is characterized by strong wind shear (SWS) and a humid atmosphere, also shown in Table 1. Therefore, two important factors in aerosol-DCC interactions: wind shear and RH are identified. Furthermore, case 6 has low convective available potential energy (CAPE) (about 1000 J kg$^{-1}$), while case 8 represents a high CAPE case of a value about 2070 J kg$^{-1}$, the highest CAPE among all eight cases.

**Table 2.** Sensitivity Studies for Case 6 and Case 8

| Case 6 | | Case 8 |
|---|---|---|
| | *Switch Wind Shear* | |
| WWS and dry[a] | | SWS and humid[a] |
| SWS and dry | | WWS and humid |
| | *Change RH* | |
| WWS and humid[b] | | SWS and dry [c] |
| SWS and humid | | WWS and dry |

[a]Original case parameters.
[b]Increased by 10%.
[c]Decreased by 10%.

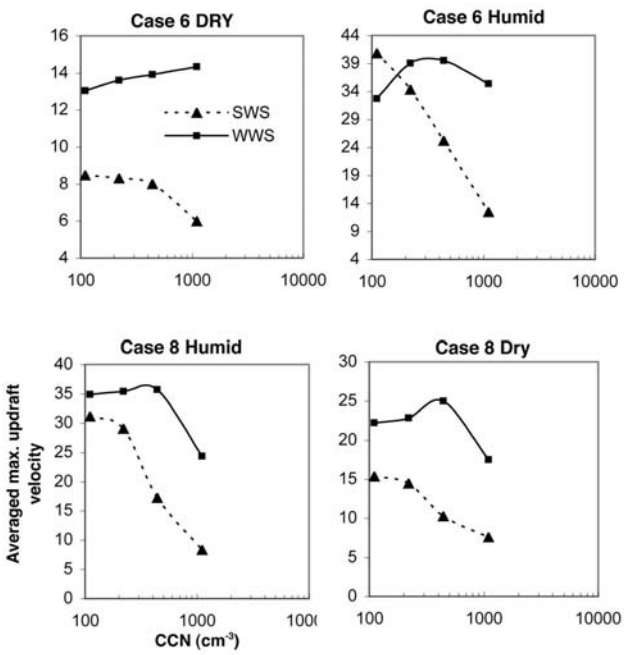


**Figure 2.** Averaged maximum updraft velocities over the time steps during cloud developing stages versus CCN concentrations for cases 6 and 8 under both dry and humid conditions. The solid and dashed curves denote WWS and SWS, respectively.

[13] More experiments were then designed to examine the relative importance of these two identified factors. On the basis of the two representative cases (cases 6 and 8), we created four soundings for each case by exchanging the wind shear profiles and changing RH as shown in Table 2. As a result, for case 6, we have the following four sounding conditions: dry (original) with WWS (original), dry with SWS (from case 8), humid (by increasing original RH by 10%) with WWS, and humid with SWS (from case 8). For case 8, four soundings are humid (original) and SWS (original), humid and WWS (from case 6), dry (decreased RH by 10%) and SWS, and dry and WWS. As mentioned in section 2.2, four CCNC levels from clean to polluted conditions were run for each sounding condition to simulate aerosol effects.

[14] A dominant role of the wind shear is noted immediately by examining the dependence of convection strength of the isolated DCCs on aerosols during cloud developing stages (cloud developing stage is defined as the time period from the start of the convection to the maximum updraft velocity) in Figure 2. Wind shear condition qualitatively separates aerosol effects on DCC convective strength into two regimes. Under WWS, the updraft velocity increases with CCNC and an optimum CCNC was around 500 $cm^{-3}$, except for case 6 with the original sounding, where optimum CCNC is higher. This response of convective strength to CCNC under WWS is in line with results by both *Rosenfeld et al.* [2008] and *Koren et al.* [2008]. However, under SWS the response pattern of updraft velocity to CCNC no longer holds: the updraft velocity always decreases with increasing CCNC and the decreasing rate is greater when the atmosphere is more humid. We also note an expected increase in convection strength with RH since the convective available potential energy (CAPE) increases dramatically with RH [*Fan et al.*, 2007b]. This increase with RH is nearly canceled under SWS by the suppressing effect of aerosols when CCNC is high. Since the suppression of convective strength by aerosols under strong wind shear and the invigoration of convection under weak wind

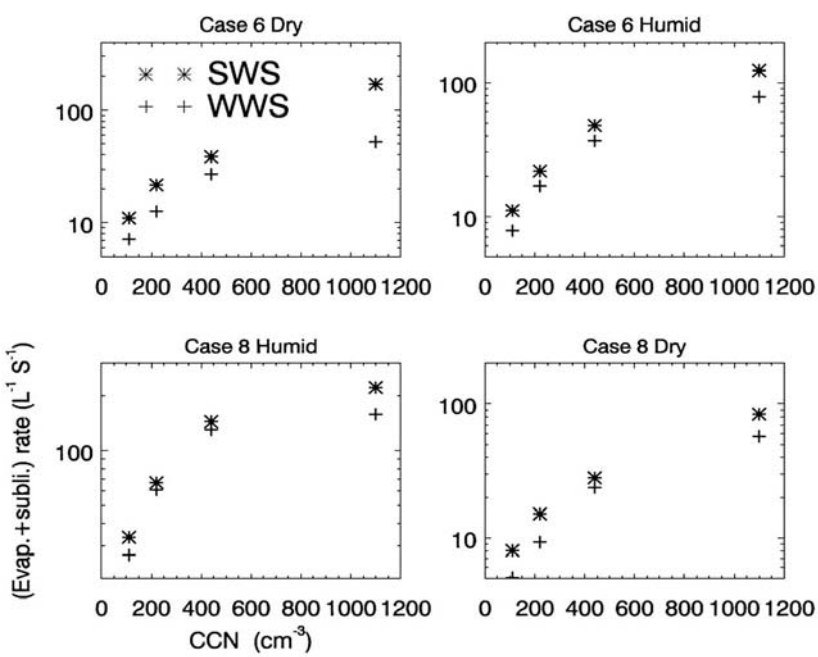


**Figure 3.** Averaged evaporation and sublimation rates over the cloudy points during cloud developing stages for cases 6 and 8 under both dry and humid conditions (plus denotes WWS and star symbol denotes SWS).

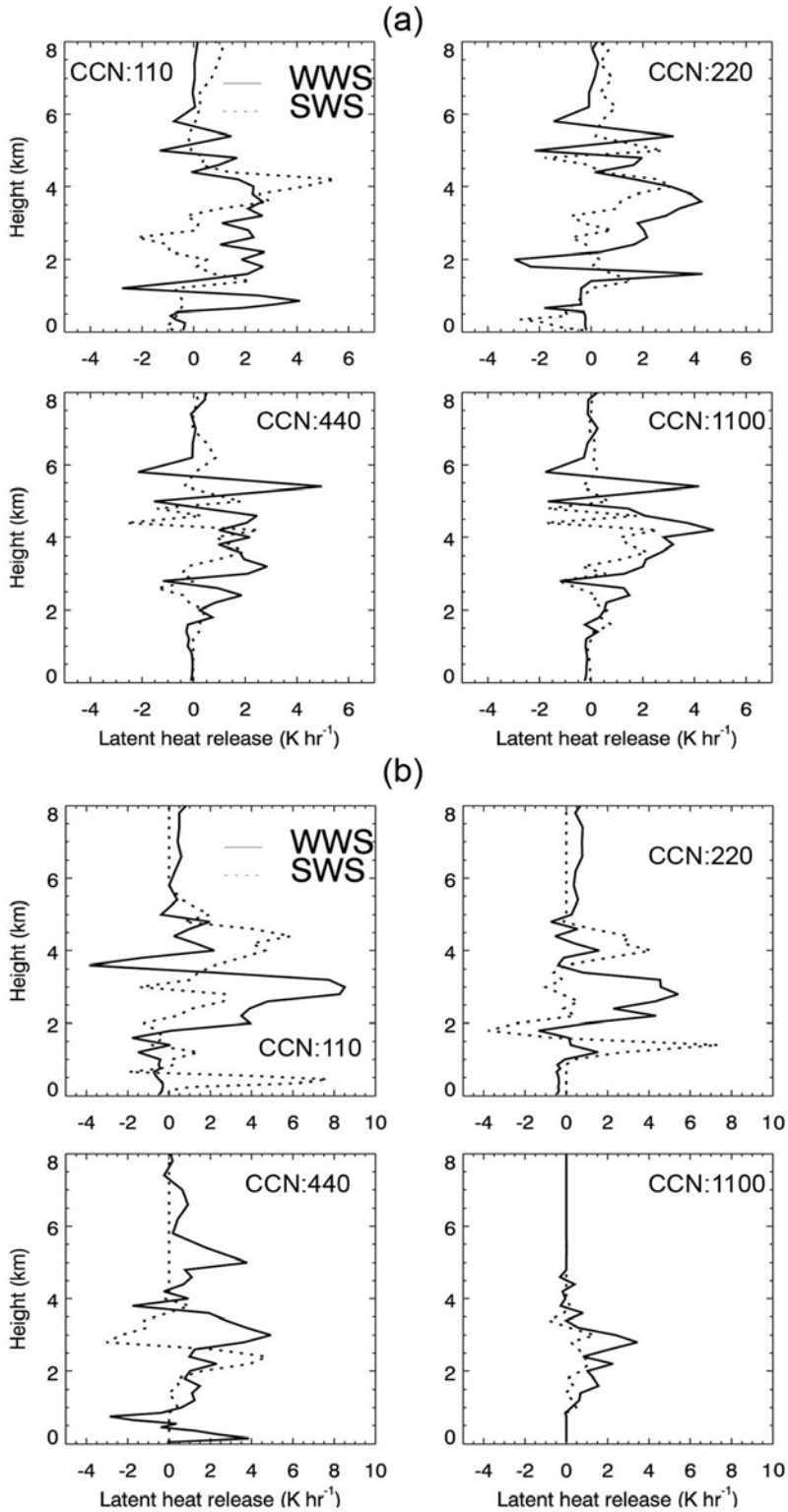


**Figure 4.** Net latent heat profiles averaged over the convective core areas (10 km domain centered at the maximum updraft velocity) during cloud developing stages for (a) case 6 (dry and WWS) and (b) case 8 (humid and SWS) with four CCN concentrations at 110, 220, 440, and 1100 cm$^{-3}$. The solid and dashed curves denote WWS and SWS, respectively.

**Table 3.** Averaged Net Latent Heat Release Over the Profiles Obtained as Those in Figure 4[a]

| CCNC ($cm^{-3}$) | Case 6 Dry | | Case 6 Humid | | Case 8 Dry | | Case 8 Humid | |
|---|---|---|---|---|---|---|---|---|
| | Weak Wind | Strong Wind | Weak Wind | Strong Wind | Weak Wind | Strong Wind | Weak Wind | Strong Wind |
| 110 | 0.52 | 0.25 | 4.20 | 2.72 | 0.78 | 0.15 | 0.43 | 0.71 |
| 220 | 0.52 | 0.22 | 4.35 | 2.52 | 0.81 | 0.13 | 0.54 | 0.22 |
| 440 | 0.55 | 0.11 | 4.63 | 2.02 | 2.61 | 0.07 | 0.62 | 0.097 |
| 1100 | 0.50 | 0.10 | 4.15 | 0.17 | 0.36 | 0.014 | 0.24 | 0.074 |

[a]The unit for net latent heat release is K $h^{-1}$.

shear are seen in both cases with low and high CAPE values, respectively, the buoyant energy would not be an important factor responsible for our result. In addition, the initial heat perturbation should also be excluded as a factor since the same initial perturbation was used for the sensitivity tests of wind shear and CCN on each case.

[15] To explain these results, we first examined the sum of the droplet evaporation and ice sublimation rate under SWS and WWS as shown in Figure 3. The average rate is always higher under SWS for each CCNC and the difference between SWS and WWS increases with CCNC. For example, in case 6 (dry), the differences in evaporation and sublimation rates between SWS and WWS are 4, 9, 13, and 118 $L^{-1}$ $s^{-1}$, corresponding to CCNC increasing from 110 to 1100 $cm^{-3}$. Strong wind shear within the cloud layer ventilated cloud particles [*Khain*, 2009] and low-level wind shear dispersed cloud developing core and enhanced entrainment [*Fedorovich and Conzemius*, 2008], both of which result in higher evaporation and sublimation rates and then larger evaporative cooling, contributing to severely reduced convection strength under SWS. *Khain et al.* [2005] also indicated that shear enhanced evaporative cooling led to a decrease in precipitation for isolated storms developing in polluted air.

[16] We further inspect the net latent heat release profile, the energy source for convection. The net latent heat release is the sum of condensational heating and evaporative cooling. Figure 4 presents the net latent heat profiles for case 6 and case 8 under original RH and wind shear conditions, i.e., dry and WWS for case 6 and humid and SWS for case 8. Generally, the net latent heat release is larger under WWS relative to SWS for each CCNC in both a humid and dry atmosphere, especially for the layer at 2–4 km, where clouds originate. By examining the net latent heat release trend, we find that it decreases significantly as CCNC increases under SWS. However, it increases under WWS until an optimum CCNC is reached. The net latent heat release averaged over the vertical profile presented in Table 3 also shows the similar trend. For example, for case 8 under a relatively dry condition, the averaged net latent heat release under SWS are 0.15, 0.13, 0.07, and 0.02 K $h^{-1}$, corresponding to CCNC increasing from 110 to 1100 $cm^{-3}$. Under WWS, the corresponding values are 0.78, 0.81, 2.61, and 0.36 K $h^{-1}$, where a significant decrease does not occur until CCNC reaches 1100 $cm^{-3}$. As CCNC increases, both condensational heating and evaporative cooling can increase. Under WWS, the increase rate of condensational heating can be higher than that of evaporative cooling with increasing CCN, leading to an increase in net latent heat release and then the enhancement of convection by aerosols. The optimal CCNC is obtained when the increase of condensational heating is balanced by the increase of evaporative cooling. However, under SWS, increasing CCNC always leads to a larger increase in evaporation and sublimation than in condensation and deposition, which results in the decreased net latent heat release and then the suppression of convection by aerosols. Comparing the net latent heat release under the dry conditions with that under the relative humid conditions shown in Figure 4, we also find that under SWS, reduction in the net latent heat release by aerosols is larger when the atmosphere is more humid, explaining why the suppressing effect of aerosols is the most prominent under the SWS and humid conditions.

[17] In addition, we examined the simulated surface precipitation rates from DCCs (Figure 5), another important quantity determined largely by convective strength. The changes of averaged surface precipitation rates with increasing CCNC under SWS and WWS are similar to the patterns of updraft velocity shown in Figure 2. This further indicates the robustness of our finding about the dominant role that wind shear plays in the suppression or invigoration of convection by aerosols. Since surface precipitation rate affects runoffs and groundwater resources, our finding has significant

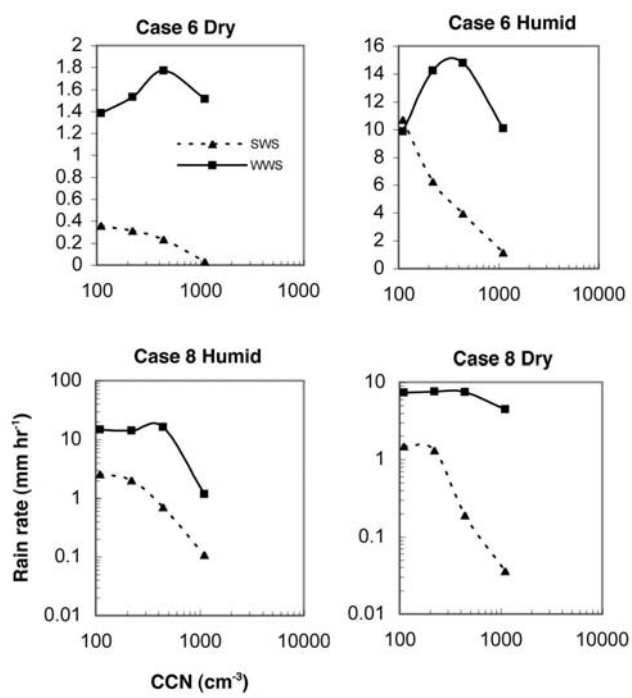


**Figure 5.** Averaged surface precipitation rates versus CCN concentrations over the grids with surface rain rate larger than 0 mm $h^{-1}$ during the period from the beginning of the simulation to 30 min after the maximum convective strength for case 6 and case 8 under both dry and humid conditions.

implications for aerosol effects on precipitation and the hydrological cycle locally. It may add another important dimension to the picture on how wind shear can regulate aerosol effects on DCCs, which was nicely summarized by *Khain* [2009, Figure 11].

[18] In a separate study (J. Fan, J. Comstock, M. Ovtchinnikov, and S. A. McFarlane, Dominant effects of CCN over IN on tropical anvil properties and water vapor content of Tropical Tropopause Layer (TTL), manuscript in preparation, 2009), 3-D cloud-resolving simulations were run for two isolated deep convective cloud cases developed in the contrasting environments, i.e., humid with WWS and dry with SWS, respectively. Aerosols enhanced convection in the case with WWS and suppressed convection in the case with SWS, agreeing with and supporting our findings from the 2-D simulations in this study.

## 4. Conclusions and Discussion

[19] We have systematically assessed the aerosol effects on convection for isolated DCCs under various dynamic and thermodynamic environments with cloud-resolving model simulations coupled with detailed spectral bin microphysics. A dominant role by vertical wind shear in regulating aerosol effects on DCCs is discovered. Generally, aerosols suppress convective strength in the case of strong wind shear; the decreasing rate of convective strength with increasing aerosols is greater in the humid air than that in the dry air. However, under weak wind shear conditions, aerosols enhance convection until an optimum of aerosol loading is reached. The main reason is that the increase in condensational heating can be larger than the increase in evaporative cooling as aerosols increase under the weak wind shear conditions, leading to the increase of net latent heat release and then the stronger convection until they are balanced (i.e., an optimal CCN is reached). With strong wind shear, however, the increase in evaporative cooling is always larger than the increase in condensational heating with increasing aerosols, leading to the suppression of convection. Our literature survey also suggests that pollution tends to invigorate single DCCs under weak wind shear conditions [*Fan et al.*, 2007b; *Zhang et al.*, 2007; *van den Heever et al.*, 2006; *Li et al.*, 2008] while the opposite occurs under strong wind shear [*Rosenfeld*, 1999; *Khain et al.*, 2004; *Khain et al.*, 2008].

[20] It is noted that wind shear was found to have another role in regulating aerosol effects on DCCs for squall lines [*Tao et al.*, 2007] and cloud ensembles [*Lee et al.*, 2008]. The evaporative cooling enhanced by wind shear could enhance precipitation by secondary cloud formation through a stronger cold pool. This dynamic feedback can contribute to increased total convective area and precipitation [*Tao et al.*, 2007; *Khain*, 2009]. Therefore, we stress that our results may only be applicable to isolated storms. We are also aware that wind shear effect on convection varies with the vertical location and thickness of shears [*Robe and Emanuel*, 2001], which can be examined further in future sensitivity studies.

[21] Nevertheless, we highlight the role of wind shear in qualitatively regulating aerosol effects on isolated DCCs. Efforts have been made to incorporate cloud microphysics into convection parameterization in general circulation models (GCM), but the entrainment rate in the parameterization is still not relevant with wind shear [*Zhang*, 2009; G. J. Zhang, personal communication, 2009]. Our results can provide the insights to better parameterize aerosol effects on convection by adding the factor of wind shear to the entrainment term, which could reduce uncertainties associated with aerosol effects on climate forcing. Our findings also suggest that aerosols have the greatest potential to suppress convection when wind shear is strong in humid areas, an effect to be explored further. All soundings in our study were taken from monsoon-affected regions. The aerosol effects on the monsoon circulation have been realized recently [*Lau et al.*, 2008; *Ramanathan et al.*, 2005], and our findings provide an important mechanism to be considered.

[22] **Acknowledgments.** This work was supported by PNNL Aerosol Climate Initiative (ACI) and grants from NASA (NNX08AH71G) and DOE (527055). A. Khain was supported by the Binational U.S.-Israel Science Foundation (BSF), grant 2006437. We thank the reviewers of the paper for their helpful comments.

## References

Ackerman, A. S., M. P. Kirkpatrick, D. E. Stevens, and O. B. Toon (2004), The impact of humidity above stratiform clouds on indirect aerosol climate forcing, *Nature*, *432*, 1014–1017, doi:10.1038/nature03174.

Albrecht, B. A. (1989), Aerosols, cloud microphysics, and fractional cloudiness, *Science*, *245*, 1227–1230, doi:10.1126/science.245.4923.1227.

Allen, G., et al. (2008), Aerosol and trace-gas measurements in the Darwin area during the wet season, *J. Geophys. Res.*, *113*, D06306, doi:10.1029/2007JD008706.

Byers, H. R., and L. J. Battan (1949), Some effects of vertical wind shear on thunderstorm structure, *Bull. Am. Meteorol. Soc.*, *30*, 168–175.

Ekman, A. M. L., A. Engström, and C. Wang (2007), The effect of aerosol composition and concentration on the development and anvil properties of a continental deep convective cloud, *Q. J. R. Meteorol. Soc.*, *133*, 1439–1452.

Fan, J., R. Zhang, G. Li, W.-K. Tao, and X. Li (2007a), Simulations of cumulus clouds using a spectral microphysics cloud-resolving model, *J. Geophys. Res.*, *112*, D04201, doi:10.1029/2006JD007688.

Fan, J., R. Zhang, G. Li, and W.-K. Tao (2007b), Effects of aerosols and relative humidity on cumulus clouds, *J. Geophys. Res.*, *112*, D14204, doi:10.1029/2006JD008136.

Fan, J., M. Ovtchinnikov, J. Comstock, S. A. McFarlane, and A. Khain (2009), Ice formation in Arctic mixed-phase clouds: Insights from a 3-D cloud-resolving model with size-resolved aerosol and cloud microphysics, *J. Geophys. Res.*, *114*, D04205, doi:10.1029/2008JD010782.

Fedorovich, E., and R. Conzemius (2008), Effects of wind shear on the atmospheric convective boundary layer structure and evolution, *Acta Geophys.*, *56*, 114–141, doi:10.2478/s11600-007-0040-4.

Schoenberg Ferrier, B., J. Simpson, and W.-K. Tao (1996), Factors responsible for precipitation efficiencies in midlatitude and tropical squall simulations, *Mon. Weather Rev.*, *124*, 2100–2125, doi:10.1175/1520-0493(1996)124<2100:FRFPEI>2.0.CO;2.

Guo, H., Y. Liu, and J. E. Penner (2008), Does the threshold representation associated with the autoconversion process matter?, *Atmos. Chem. Phys.*, *8*, 1225–1230.

Kaufman, Y. J., I. Koren, L. A. Remer, D. Rosenfeld, and Y. Rudich (2005), The effect of smoke, dust, and pollution aerosol on shallow cloud development over the Atlantic ocean, *Proc. Natl. Acad. Sci. U. S. A.*, *102*, 11,207–11,212, doi:10.1073/pnas.0505191102.

Khain, A. P. (2009), Notes on state-of-art investigations of aerosol effects on precipitation: A critical review, *Environ. Res. Lett.*, *4*, 015004, doi:10.1088/1748-9326/4/1/015004.

Khain, A. P., and A. Pokrovsky (2004), Simulation of effects of atmospheric aerosols on deep turbulent convective clouds using a spectral microphysics mixed-phase cumulus cloud model. Part II: Sensitivity study, *J. Atmos. Sci.*, *61*, 2983–3001, doi:10.1175/JAS-3281.1.

Khain, A. P., M. Ovtchinnikov, M. Pinsky, A. Pokrovsky, and H. Krugliak (2000), Notes on the state-of-the-art numerical modeling of cloud microphysics, *Atmos. Res.*, *55*, 159–224, doi:10.1016/S0169-8095(00)00064-8.

Khain, A., A. Pokrovsky, M. Pinsky, A. Seifert, and V. Phillips (2004), Simulation of effects of atmospheric aerosols on deep turbulent convec-

tive clouds using a spectral microphysics mixed-phase cumulus cloud model. Part II: Sensitivity study, *J. Atmos. Sci.*, *61*, 2963–2982, doi:10.1175/JAS-3350.1.

Khain, A., D. Rosenfeld, and A. Pokrovsky (2005), Aerosol impact on the dynamics and microphysics of deep convective clouds, *Q. J. R. Meteorol. Soc.*, *131*, 2639–2663, doi:10.1256/qj.04.62.

Khain, A., N. BenMoshe, and A. Pokrovsky (2008), Factors determining the impact of aerosols on surface precipitation from clouds: An attempt at classification, *J. Atmos. Sci.*, *65*, 1721–1748, doi:10.1175/2007JAS2515.1.

Khairoutdinov, M. F., and D. A. Randall (2003), Cloud resolving modeling of the ARM summer 1997 IOP: Model formulation, results, uncertainties, and sensitivities, *J. Atmos. Sci.*, *60*, 607–625, doi:10.1175/1520-0469(2003)060<0607:CRMOTA>2.0.CO;2.

Khairoutdinov, M. F., and D. A. Randall (2006), High-resolution simulation of shallow-to-deep convection transition over land, *J. Atmos. Sci.*, *63*, 3421–3436, doi:10.1175/JAS3810.1.

Khvorostyanov, V. I., and J. A. Curry (2000), A new theory of heterogeneous ice nucleation for application in cloud and climate models, *Geophys. Res. Lett.*, *27*, 4081–4084, doi:10.1029/1999GL011211.

Koren, I., J. V. Martins, L. A. Remer, and H. Afargan (2008), Smoke invigoration versus inhibition of clouds over the Amazon, *Science*, *321*, 946–949, doi:10.1126/science.1159185.

Lau, K., et al. (2008), The Joint Aerosol-Monsoon Experiment: A new challenge for monsoon climate research, *Bull. Am. Meteorol. Soc.*, *89*, 369–383, doi:10.1175/BAMS-89-3-369.

Lee, S. S., L. J. Donner, V. T. J. Phillips, and Y. Ming (2008), The dependence of aerosol effects on clouds and precipitation on cloud-system organization, shear and stability, *J. Geophys. Res.*, *113*, D16202, doi:10.1029/2007JD009224.

Levin, Z., and W. Cotton (Eds.) (2008), *Aerosol Pollution Impact on Precipitation: A Scientific Review*, Springer, New York.

Li, G., Y. Wang, and R. Zhang (2008), Implementation of a two-moment bulk microphysics scheme to the WRF model to investigate aerosol-cloud interaction, *J. Geophys. Res.*, *113*, D15211, doi:10.1029/2007JD009361.

Lin, J. C., T. Matsui, R. A. Pielke Sr., and C. Kummerow (2006), Effects of biomass-burning-derived aerosols on precipitation and clouds in the Amazon Basin: A satellite-based empirical study, *J. Geophys. Res.*, *111*, D19204, doi:10.1029/2005JD006884.

Liu, Y., and P. H. Daum (2002), Indirect warming effect from dispersion forcing, *Nature*, *419*, 580–581, doi:10.1038/419580a.

Liu, Y., P. H. Daum, R. McGraw, and M. Miller (2006), Generalized threshold function accounting for effect of relative dispersion on threshold behavior of autoconversion process, *Geophys. Res. Lett.*, *33*, L11804, doi:10.1029/2005GL025500.

Liu, Y., P. H. Daum, H. Guo, and Y. Peng (2008), Dispersion bias, dispersion effect, and the aerosol-cloud conundrum, *Environ. Res. Lett.*, *3*, 045021, doi:10.1088/1748-9326/3/4/045021.

Lu, M.-L., W. C. Conant, H. H. Jonsson, V. Varutbangkul, R. C. Flagan, and J. H. Seinfeld (2007), The Marine Stratus/Stratocumulus Experiment (MASE): Aerosol-cloud relationships in marine stratocumulus, *J. Geophys. Res.*, *112*, D10209, doi:10.1029/2006JD007985.

National Research Council (2005), *Radiative Forcing of Climate Change: Expanding the Concept and Addressing Uncertainties*, Natl. Acad. Press, Washington, D. C.

Ramanathan, V., et al. (2005), Atmospheric brown clouds: Impacts on South Asian climate and hydrological cycle, *Proc. Natl. Acad. Sci. U. S. A.*, *102*, 5326–5333, doi:10.1073/pnas.0500656102.

Richardson, Y., and K. Droegemeier (2007), The influence of horizontal environmental variability on numerically simulated convective storms. Part I: Variations in vertical shear, *Mon. Weather Rev.*, *135*, 3429–3455, doi:10.1175/MWR3463.1.

Robe, F. R., and K. A. Emanuel (2001), The effect of vertical wind shear on radiative-convective equilibrium states, *J. Atmos. Sci.*, *58*, 1427–1445, doi:10.1175/1520-0469(2001)058<1427:TEOVWS>2.0.CO;2.

Rosenfeld, D. (1999), TRMM observed first direct evidence of smoke from forest fires inhibiting rainfall, *Geophys. Res. Lett.*, *26*, 3105–3108, doi:10.1029/1999GL006066.

Rosenfeld, D. (2000), Suppression of rain and snow by urban and industrial air pollution, *Science*, *287*, 1793–1796, doi:10.1126/science.287.5459.1793.

Rosenfeld, D., U. Lohmann, G. B. Raga, C. D. O'Dowd, M. Kulmala, S. Fuzzi, A. Reissell, and M. O. Andreae (2008), Flood or drought: How do aerosols affect precipitation?, *Science*, *321*, 1309–1313, doi:10.1126/science.1160606.

Rudich, Y., D. Rosenfeld, and O. Khersonsky (2002), Treating clouds with a grain of salt, *Geophys. Res. Lett.*, *29*(22), 2060, doi:10.1029/2002GL016055.

Sassen, K., P. J. Demott, J. M. Prospero, and M. R. Poellet (2003), Saharan dust storms and indirect aerosol effects on clouds: CRYSTAL-FACE results, *Geophys. Res. Lett.*, *30*(12), 1633, doi:10.1029/2003GL017371.

Smolarkiewicz, P. K., and W. W. Grabowski (1990), The multidimensional positive definite advection transport algorithm: Nonnoscillatory option, *J. Comput. Phys.*, *86*, 355–375, doi:10.1016/0021-9991(90)90105-A.

Takemi, T. (2007), A sensitivity of squall-line intensity to environmental static stability under various shear and moisture conditions, *Atmos. Res.*, *84*, 374–389, doi:10.1016/j.atmosres.2006.10.001.

Tao, W.-K., X. Li, A. Khain, T. Matsui, S. Lang, and J. Simpson (2007), Role of atmospheric aerosol concentration on deep convective precipitation: Cloud-resolving model simulations, *J. Geophys. Res.*, *112*, D24S18, doi:10.1029/2007JD008728.

Teller, A., and Z. Levin (2006), The effects of aerosols on precipitation and dimensions of subtropical clouds: A sensitivity study using a numerical cloud model, *Atmos. Chem. Phys.*, *6*, 67–80.

van den Heever, S. C., G. G. Carrio, W. R. Cotton, P. J. DeMott, and A. J. Prenni (2006), Impact of nucleating aerosol on Florida storms, part 1: Mesoscale simulations, *J. Atmos. Sci.*, *63*, 1752–1775, doi:10.1175/JAS3713.1.

Wang, C. (2005), A modeling study of the response of tropical deep convection to the increase of cloud condensation nuclei concentration: 1. Dynamics and microphysics, *J. Geophys. Res.*, *110*, D21211, doi:10.1029/2004JD005720.

Yuan, T., Z. Li, R. Zhang, and J. Fan (2008), Increase of cloud droplet size with aerosol optical depth: An observation and modeling study, *J. Geophys. Res.*, *113*, D04201, doi:10.1029/2007JD008632.

Zhang, G. J. (2009), Effects of entrainment on convective available potential energy and closure assumptions in convection parameterization, *J. Geophys. Res.*, *114*, D07109, doi:10.1029/2008JD010976.

Zhang, R., G. Li, J. Fan, D. L. Wu, and M. J. Molina (2007), Intensification of Pacific storm track linked to Asian pollution, *Proc. Natl. Acad. Sci. U. S. A.*, *104*, 5295–5299, doi:10.1073/pnas.0700618104.

J. M. Comstock, J. Fan, S. Ghan, L. R. Leung, and M. Ovchinnikov, Climate Physics Group, Pacific Northwest National Laboratory, P.O. Box 999, MSIN k9-24, Richland, WA 99352, USA. (jiwen.fan@pnl.gov)

A. Khain, Institute of the Earth Science, Hebrew University of Jerusalem, Givat Ram, Jerusalem 91904, Israel.

Z. Li, Department of Atmospheric and Oceanic Sciences, University of Maryland at College Park, College Park, MD 20740, USA.

V. J. Martins and T. Yuan, Joint Center for Earth Systems Technology, University of Maryland Baltimore County, 5523 Research Park Dr., Baltimore, MD 21228, USA.